



Zinc Oxide nano-rods: Challenges for Glucose Biosensors

Hanan A. Wahab,^a Aziza A. El Saeid,^b Aida A. Salama,^b Inas K. Battisha,^{a*}

^a*Solid State Physics Department, Physics Research Division, National Research Centre (NRC), 33 El Behooth St., Dokki, Giza, Egypt, (Affiliation ID: 60014618).*

^b*Physics Department, Faculty of Science, AL Azhar University (Girls), Cairo, Egypt*



CrossMark

Abstract

Zinc oxide nano-rod thin films (ZnR) will be deposited on silicon substrate ($ZnRS$) and borosilicate glass capillary tube tip (0.5 and 0.7 μm as inner and outer diameters, respectively) ($ZnRT$) using both Sol-Gel (SG) and aqueous chemical growth (ACG) techniques for glucose biosensor fabrication. It will be functionalized with membranes or enzymes to produce selective glucose biosensor for glucose concentration measurements in extracellular solutions. The prepared thin film samples provided a favourable environment for the glucose oxidase (GOD) immobilization and introduced a shuttling way for electronic communication between electrodes and GOD. The prepared $ZnRS$ and $ZnRT$ structures and morphologies will be characterized by X-ray diffraction (XRD) and Field emission high resolution scanning electron microscopy (FESEM).

Keywords: $ZnRS$; $ZnRT$; Sol-Gel; Glucose biosensors.

1. Introduction

Glucose is one of the most important studied analytes due to its immense importance in the human body and medicine and it is one of the main products of the human body's primary energy source. Where diseases such as diabetes could be developed if glucose levels in the blood are not properly regulated. For blood-glucose monitoring importance, significant research has been focusing to produce reliable methods [1-2]. Molecular modeling was utilized to investigate its electronic as well as structural properties [3-4]. ZnO nano-rods thin film has many advantages for using it as biosensor material, it has generated keen interest in biosensors due to its enormous useful properties, where it shows n-type semiconducting property and that their electrical transport is highly dependent on the chemical species adsorption/desorption nature. It has small size, possesses polar surface, being bio-safe. Moreover, ZnO is non-toxic; it has electrochemical activity, chemical stability, and has high electron communication features [5]. For ZnO nano-rods thin film preparation, sol-gel and aqueous chemical growth method are to be used. Various techniques for ZnO nano-particles preparation have been applied: sol-gel method, co-precipitation method etc. Among the different methods, the sol-gel approach appears to be one of the most promising methods to prepare ZnO nano-particles. Some of the most important sol-gel method advantages are: the synthesis

easiness, low temperature of decomposition and control on the chemical composition. These advantages make the sol-gel technique a very attractive preparation method [6]. During the last few years, electrochemical biosensors have been great interest for glucose concentrations detection. Electrochemical biosensors based on Zinc Oxide nano-rods (potentiometric, conductometric, impedometric and amperometric) are widely employed for intra/extracellular glucose sensing [7-12]. It is providing an attractive means to analyze the biological sample content owing to the direct conversion biological event to an electric signal. Electrochemical measurements with ZnO nano-rods-based biosensors prepared by both sol-gel and aqueous chemical growth techniques [13-16]. when the test solution composition was altered the electrochemical cell voltage (electromotive force) was changed. These changes can be related to the concentration of glucose ions in the test solution via a calibration procedure [17].

It is well known that the glucose is commonly oxidized by enzymes. Enzymes are biological recognition molecules commonly used in development and research due to that most chemical reactions in living systems are catalyzed by own specific enzymes [18-19]. As a consequence, enzymes immobilization strategies are important to preserve their biological activity [20-23]. Glucose biosensors are based on the glucose recognition by the enzyme glucose oxidase (GOD). In glucose biosensors the mentioned enzyme is

*Corresponding author e-mail: szbasha@yahoo.com; (Inas K. Battisha).

Receive Date: 30 December 2020, Revise Date: 06 January 2021, Accept Date: 15 January 2021

DOI: 10.21608/EJCHEM.2021.55880.3191

©2021 National Information and Documentation Center (NIDOC)

widely employed due to its stability and high selectivity for glucose [24–30].

For the highly selective glucose biosensors fabrication, the substrate choice for dispersing the sensing material decides the sensor performance. Intra/extracellular glucose determination was a great interest; moreover, ZnO nano-rod thin films technology has potential for such measurements [31–34].

In the study reported here glucose oxidase was immobilized directly on Zinc Oxide nano-rods thin film deposited on silicon substrate (ZNR_S) and on borosilicate glass capillary tube tip (0.5 and 0.7 μm as inner and outer diameters, respectively) (ZNR_T), as working electrodes by electrostatic interaction. It can be used in electrochemical bio-sensing applications due to their unique advantages in combination with immobilized enzymes, their small size, high surface area to volume ratios allowing larger signals, better catalysis and the more rapid analyte movement through sensors show higher sensitivity as compared to those prepared from bulk ZnO devices. For the extra glucose concentration determination with functionalized ZNR_S and ZNR_T glucose biosensors were performed in phosphate buffer saline (PBS) over the range from 1 μM to 10 mM and in human blood plasma. The prepared samples crystal structure and surface morphologies were studied by XRD and FESEM, respectively.

The aim of the present work is to develop sensitive and selective glucose biosensor, the ZnO nano-rods grown have been used for measuring accumulating charge with no current passing through the measurement media being suitable for biological environments. This sensor will be tested in this work as an extra-cellular environment. After the extracellular measurement success, the samples were prepared for intracellular glucose detection. For that we have grown ZnO nano-rods on the tip of borosilicate glass capillaries. The main challenges have been directed to make the tip geometry small enough. Intracellular electrodes must have extremely sharp tips (sub micro meter dimensions) and they must be long (>10 μm in length). These characteristics are necessary, where new work will be done in the near future and is actually in progress now to optimize the preparation condition to be ready for effective bending and gentle penetration for the flexible cell membrane.

2. Experimental details

2.1. Preparation of Zinc Oxide nano-rods thin films (ZNR_S) and (ZNR_T)

Zinc Oxide nano-rods thin films (ZNR_{TF}) deposited on (a) silicon substrate (ZNR_S) and (b) borosilicate glass capillary tube tip (ZNR_T) (sterile Femtotip® II with tip inner diameter of 0.5 μm, tip outer diameter of 0.7 μm, and length of 49 mm.). Were prepared in two stages (seed layers and nano-rods growth using both sol-gel Technique (SG) at 250°C and aqueous chemical growth deposition techniques (ACG) at 90 – 95°C, respectively. The seed layers are used for the substrate surface modification,

where it provides nucleation sights for the nano-rod growth structures and helps to enhance the density as well as the homogeneity of particles. In addition, the seed layers provide a good control on the alignment and density of the nucleation points that affect the synthesized Zinc Oxide nano-rods diameter. Cleaning of the substrates prior to Zinc Oxide nanostructure synthesis is one of the most paramount to obtain the desired the material morphology and quality. The substrates are processed through ultrasonication in ethanol solution for 15 minutes and then in de-ionized water. This process helps to remove dust and unwanted chemicals from the surface of the substrate and provides a clean surface which can be used for further procedure. A coating seed solution was prepared by dissolving Zinc acetate dehydrate ($Zn(CH_3COO)_2 \cdot 2H_2O$) in mixed solution of mono-ethanolamine ($NH_2CH_2CH_2OH$) MEA and 2-methoxyethanol at room temperature (about 25°C), Then it was stirred at 50°C for 2 h until yielding a clear and homogeneous solution. The mixed solutions were aged at room temperature for another 24 h [10].

For seed layers preparation by using sol-gel method to obtain the desired morphology and good quality of the prepared material, the substrate was cleaned prior to nano-crystal ZnO thin film deposition as reported previously by our team work [10 & 13]. The mentioned mixed solution was used for coating on the (ZNR_S) by using the spin coater with a speed of 3000 rpm for 30 sec. The same solution was coated on the (ZNR_T) by a simple dip coating method to obtain nano-crystalline ZnO (seed layers) all around the tip surface. The coating process was repeated several time and dried in open air at room temperature and finally placed in pre-heated laboratory oven at 250°C for annealing in order to decompose the zinc acetate dehydrate into ZnO nano-particles. In addition, the seed solution prepared by using sol gel technique provides a good control on the alignment and density of the nucleation points that affect the diameter of the synthesized nano-structure. After uniformly coating the substrates with Zinc Oxide seed layers, the Zinc Oxides nano-rods growth was achieved by immersing both (ZNR_S) and (ZNR_T) Zinc Oxides seed-layer in 150 mL of [0.025 M Zinc nitrate ($Zn(NO_3)_2$) and 0.025 M hexamethylenetetramine (HMT, $C_6H_{12}N_4$)] aqueous solution using ACG method. The ACG reaction temperature was kept at 90 – 95°C for 4–6 h. Finally, the substrate was removed from the solution, then immediately rinsed in de-ionized water to remove any residual salt from the surface and dried in air at room temperature.

2.2. Methods

2.2.1. Sol-Gel technique

The sol-gel process is a wet-chemical technique widely used in the fields of material science and ceramic engineering. Such methods are used primarily for the fabrication of materials (metal oxides) starting from a colloidal solution (sol) that acts as the precursor for an

integrated network (or gel) of either discrete particles or network polymers. The Sol is made of solid particles of a diameter of few hundred of nm suspended in a liquid phase. Then the particles condense in a new phase (gel) in which solid is immersed in a liquid phase (solvent). The precursors are metal, alkoxides and metal salts (such as chlorides, nitrates and acetates), which undergo various forms of hydrolysis and poly-condensation reactions.

- Sol-Gel Coating Techniques

A sol is a dispersion of the solid particles (~ 0.1-1 μm) in a liquid where only the Brownian motions suspend the particles. A gel is a state where both liquid and solid are dispersed in each other, which presents a solid network containing liquid components. The sol-gel coating process usually consists of 4 steps:

- (1) The desired colloidal particles once dispersed in a liquid to form a sol.
- (2) The deposition of sol solution produces the coatings on the substrates by spraying, dipping or spinning.
- (3) The particles in sol are polymerized through the removal of the stabilizing components and produce a gel in a state of a continuous network.
- (4) The final heat treatments pyrolyze the remaining organic or inorganic components and form an amorphous or crystalline coating [35-36].

There are two distinct reactions in the sol-gel process: hydrolysis of the alcohol groups and condensation of the resulting hydroxyl groups.

-Advantages of Sol-Gel Technique

- * Can produce thin bond-coating to provide excellent adhesion between the metallic substrate and the top coat.
- * Can produce thick coating to provide corrosion protection performance.
- * Can easily shape materials into complex geometries in a gel state
- * Can produce high purity products because the organo-metallic precursor of the desired ceramic oxides can be mixed, dissolved in a specified solvent and hydrolysed into a sol, and subsequently a gel, the composition can be highly controllable.
- * Can have low temperature sintering capability, usually 200-600°C.
- * Can provide a simple, economic and effective method to produce high quality coatings.

The sol gel process has proved to be an excellent method for the preparation of many types of optical coatings, of the many potential coating method available, only three have the capability of lying down very thin layers of precise thickness. These are spin and dip coating, which are the most widely used, and meniscus coating, which is comparatively new.

2.2.2 Aqueous chemical growth (ACG) method

:

The aqueous chemical growth is one of the techniques that have been extensively employed, where it is the most simple, cheap and effective method to synthesize different metal oxide nanostructures. The term aqueous chemical stands for the heterogeneous reactions occurred in the presence of aqueous solvents/minerals. Some of its advantages are low temperature, low manufacturing cost, simple equipment, superior throughput, in-situ doping and environment friendly.

Most importantly by using aqueous chemical growth method variety of metal oxide nanostructures can easily be grown on different substrates like metal surface, semiconductors, glass, plastic, common paper, aluminium foil, grapheme and cotton textile.

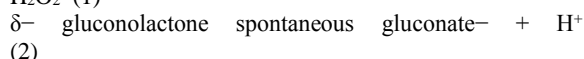
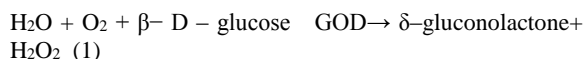
2.2.3 Biosensor Technique

For ZnO nano-rods - based glucose electrochemical biosensors fabrication, it will be deposited on the two mentioned substrate kinds. However, they will be covered by Enzyme glucose Oxidase (GOD immobilization) as working electrodes.

GOD solution was prepared by using glucose Oxidase (GOD), (type x-s) From *Aspergillus Niger* by dissolving it in phosphate buffer saline (PBS) at pH 7.4 then adding glutaraldehyde solution. Before the enzymes (GOD) immobilization on the working electrode surface, the sensor working electrode was rinsed with Phosphate Buffered Saline (PBS) to generate a hydrophilic surface. To immobilize the enzymes (GOD) on ZnO nano-rods working electrodes, prepared GOD solution was deposited and left at room temperature for 2 h for drying.

Generally, all enzyme working electrodes were stored in dry condition at 4°C when not in use. After finishing these steps, the sensors were initially checked potentiometrically in tow solutions, the former is the glucose stock solution which prepared from D-(+)-glucose 99.5% and Phosphate Buffered Saline (PBS) in the range from 1 μM to 10 mM and the latter is human blood cells plasma.

The most electrochemical glucose biosensors mechanism is based on an enzymatic reaction catalyzed by GOD. As a result of this reaction, δ -gluconolactone and hydrogen peroxide (H_2O_2) are produced. These two products and the oxygen consumption can be used for the glucose determination. With the availability of H_2O_2 in the reaction, gluconolactone is spontaneously converted to gluconic acid which form the gluconate- and proton (H^+) charged products at neutral pH (about 7), according to the following two formulas given in (1) and (2).



ZnO nano-rods high surface-to-volume ratio provides a large specific surface area for the GOD adsorption, and thus comparatively more active sites for catalysis.

-Electrochemical measurements with ZnO nano-rods thin film- based glucose biosensors:

The electrochemical cell voltage (electromotive force) changed when the test electrolyte composition was altered. These changes can be related to the glucose concentration ions in the test electrolyte via a calibration procedure.

The ZnO nano-rods - based glucose biosensor electrochemical response against an Ag/AgCl reference electrode was measured at room temperature (about 25°C). PH meter (model 3510 Metrohm) was used to measure prepared glucose biosensors potentiometric output voltage.

2.3. Characterization Techniques

The resulting ZnO nano-rods thin film structures were characterized by X-ray diffraction (XRD) and Field

emission high resolution scanning electron microscope (FESEM), see details in our team work previous work [3, 8-12].

The relative dielectric permittivity was calculated using the equations:

$$\epsilon' = Cd/\epsilon_0 A \quad (3)$$

where C is the capacitance of the measured sample in Farad, d is the thickness of the thin film sample in meters, A is the cross section area of the electrode and ϵ_0 is the permittivity of free space ($8.854 \times 10^{-12} \text{ Fm}^{-1}$).

$$\epsilon'' = \epsilon' \tan \delta \quad (4)$$

where, ϵ'' is the dielectric loss and $\tan \delta$ is the loss tangent. The AC resistivity (ζ') of the prepared samples has estimated from the dielectric parameters. As long as the pure charge transport mechanism is the major contributor to the loss mechanism, ζ' can be calculated using the following relation:

$$\zeta' = 1/(\omega \epsilon_0 \epsilon' \tan \delta) \Omega \text{ Cm} \quad (5)$$

where $\omega = 2 \pi f$, ω is the angular frequency and f is the frequency of the applied electric field in Hertz.

$$\sigma = 2\pi f d C \tan \delta / A \quad (6)$$

Where σ is the A.C. conductivity, f is the operating frequency, d is the thickness of the dielectrics, $\tan \delta$ is the dielectric loss, C is the capacitance and A is the area of the electrode.

3. Results and Discussions

3.1 XRD

The ZNRs crystal structure was studied through XRD patterns by deposited seed layers sintered at 250°C, as shown in figure 1. The presented strong diffraction peak at the (002) plane, located at 34.45° indicated that Zinc Oxide sample possessed pure hexagonal wurtzite structure with high C-axis orientations; Card number [01-089-1397].

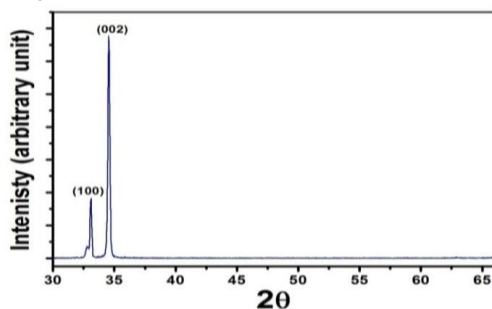


Fig. 1. XRD patterns for ZNRs with seed layers at 250°C

Among the peaks, the ZnO nano-rods prepared thin film showed the highest peak intensities on the (002) plane. Compared with the Zinc Oxide thin film standard diffraction peaks, the clear, strong and sharp peak corresponding to the ZNRs (002) crystal plan indicated that the nano-rods orientation growth along the C-axis direction possessed an excellent crystal quality, with no other diffraction peaks and/or impurities characteristic peaks. All diffraction peaks can be indexed to the ZNRs wurtzite hexagonal structure.

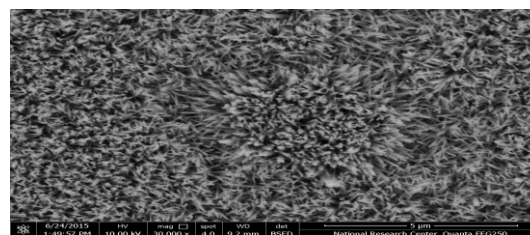
3.2 FESEM

In order to highlight on ZNRs and ZNRt surface morphologies we investigated it by using (FESEM) as shown in figure (2& 3), respectively. The Zinc Oxide nano-particles seed layers prepared samples provide the possible nucleation for the zinc oxide nano-rods growth, covering the whole area with uniform density, top surface smoothness, equal length and vertically aligned along the c-axis. ZnO nano-rods have a rod-like shape with hexagonal cross section and primarily aligned along the c-axis (perpendicular to the substrate) which corresponds well with the XRD results. The rods morphology and its nano-size control the penetration, especially in case of using the tip capillary tube substrate, when it is used as intracellular

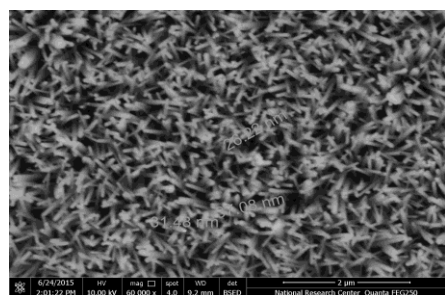
measurements, to don t damage the cell membrane of (human and / or animal). The ZnO nano-rods diameters are comparable to the size of the biological and chemical species being sensed, which intuitively makes them represent excellent primary transducers for producing electrical signals.

The obtained ZNRs FESEM images at different area and magnifications (a &b) at 30.000 x and 60.000 x respectively, are shown in figure 2 (a &b). We can observe from the figure that the ZNRs have a rod-like shape with hexagonal cross section and were distributed uniformly in diameters range between 26 and 38 nm as shown in figure 2 (b).

The ZNRt panoramic FESEM images with seed layers sintered at annealing temperature 250°C was depicted in figure 3 (a& b) at two magnifications 200x and 2000 x, respectively. It can be seen that the tip is covered with zinc oxide nano-rods at uniform density along the near perpendicular direction to the tip surface. The highly magnified FESEM images in figure 3 (c, d &e) at 24.000x, 30.000x and 60.000x, respectively displays the nano-rods shape and were found to be vertically aligned and distributed uniformly with diameter ranging from 22 up to 24.2nm. We can conclude that ZNRs and ZNRt with seed layers prepared at 250°C are very dense and highly oriented due to high seed layers annealing temperature [3, 8]. The obtained results from figure (2&3) indicated that the seed layer annealing temperature will directly influence the ZnO nano-rods formation. Adjusting the nano-particles Zinc Oxide density film is a preferable way to control the nano-rods diameter. Were the seed solution is used for the nano-rods surface modification and helps to enhance the density as well as particles homogeneity.

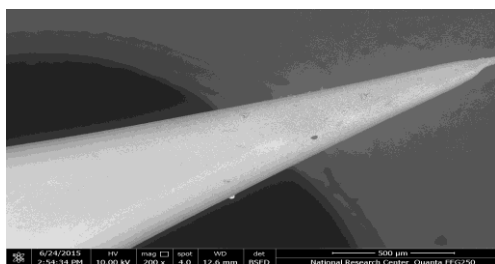


(a)

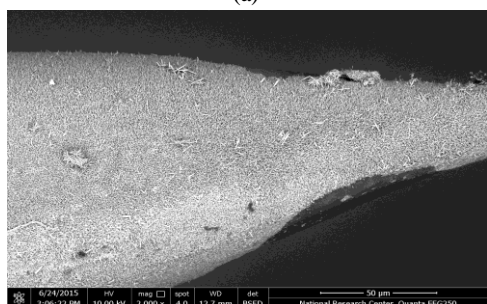


(b)

Fig. 2. (a & b) Biosensor ZN_{RS} FESEM images at different magnifications.

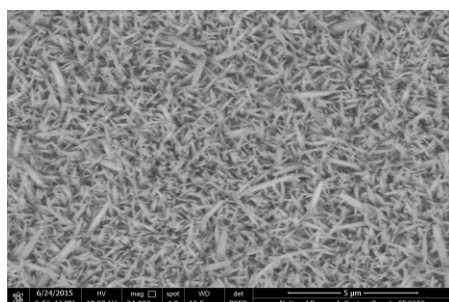


(a)

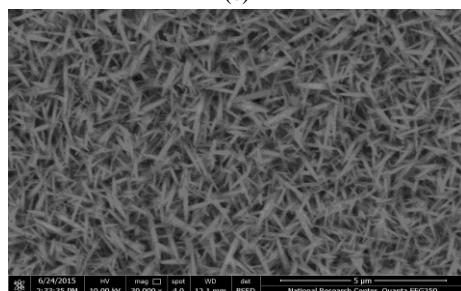


(b)

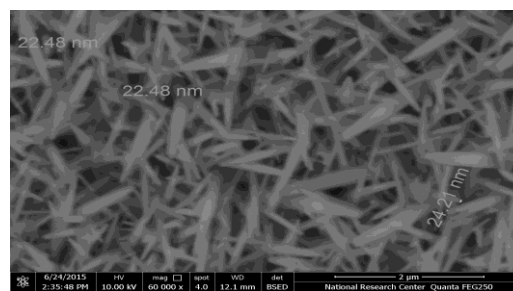
Fig. 3. (a & b) Biosensor ZN_{RT} FESEM images (a) Panoramic view, (b) focusing on small area.



(c)



(d)



(e)

Fig. 3. (c, d & e) Biosensor ZN_{RT250} FESEM images at different magnifications by focusing on small area.

3.3 Dielectric measurements

Figures (4 & 5) show the dielectric constant (ϵ') and dielectric loss (ϵ'') versus the frequency which ranging from 0.1 Hz up to 100 KHz at different temperature ranging from 30 up to 170°C for ZN_{RS} . It is clearly seen from the figures that (ϵ') and (ϵ'') are found to decrease rapidly at low frequency and decreases with substantially increasing in applied frequency until reaching nearly constant value for both of them at higher frequency.

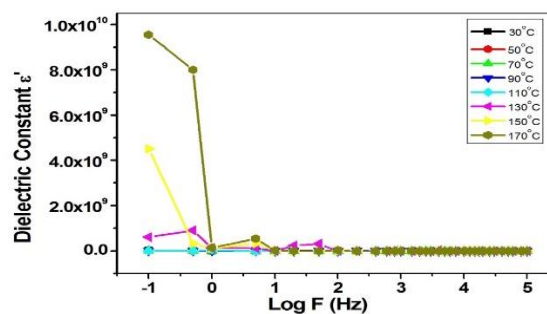


Fig. 4. The dielectric constant ϵ' as a function of log frequency for (ZN_{RS}).

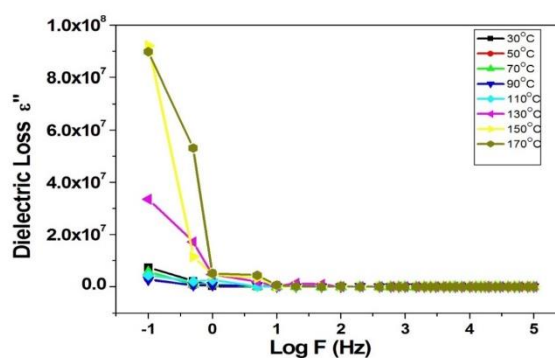


Fig. 5. The dielectric loss ϵ'' as a function of log frequency for (ZN_{RS}).

The ϵ' and ϵ'' large values at low frequencies in ZN_{RS} are due to the predominance of the vacancies species like oxygen and grain boundary defects. While the decrease with increased frequency is natural following the fact that any species contributing to polarizability is bound to show lagging behind the applied field at higher frequencies. The (ϵ') and (ϵ'') can be described by Debye dispersion relaxation mechanism. Where the dielectric constant ϵ' at

low frequency is rising by both ionic and interfacial polarization contributions. As the frequency is increased the dipoles cannot be able to rotate rapidly and follow the alternating field and ϵ' is expected to be lower as the electronic interfacial components dominate in polarization process.

Variation of ϵ' and ϵ'' in the low frequency region is due to the interfacial polarization or space charge polarization. In a nanocrystalline material, majority of atoms reside in the grain boundary or within a few atomic layers from the boundary. It is reported that the oxide materials contain oxygen vacancies. An oxygen vacancy is equivalent to a positive charge and hence possesses a dipole moment. It is expected that in nanostructure materials defect density is very high. Therefore, the $Zn_{R}S$ grain boundaries should be rich in oxygen vacancies and thereby should contain high dipoles density. Exposed to an external electric field, the dipoles will rotate leading to an increased polarization in $Zn_{R}S$, causing ϵ' high value in the low frequency regions which, can be accounted for this type of polarization.

The increase of dielectric constant ϵ' and dielectric loss ϵ'' with temperature is expected according to the hopping charge carrier's theory for polarization. The high dielectric constant ϵ' and dielectric loss ϵ'' at low frequency and high temperature can be discussed due to the permanent dipole moments presence which indicated a small effective charge separation. In general, this behaviour can be ascribed to the partially electronic polarization, which plays a significant role in this region. At relatively high temperature there are more than one polarization type are expected. This was attributed to the ionic polarization that begins to play a role in cooperation with the electronic one.

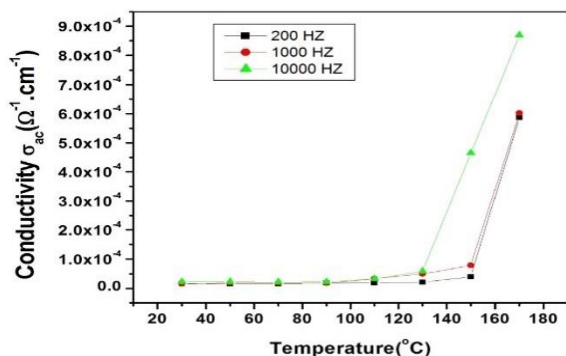


Fig. 6. The A.C. electrical conductivity versus the temperature for ($Zn_{R}S$).

Figure 6 illustrates the ac electrical conductivity a.c. (σ) dependence on temperature ranging from 30 up to 170°C for ($Zn_{R}S$) at different frequencies. It was observed that the ($Zn_{R}S$) electrical conductivity increases with increasing in temperature, reaching its maximum value at 90°C. This result informed that ($Zn_{R}S$) is highly conducted at (90°C). Thus, we can consider the temperature (90°C) is an optimum temperature degree for conductivity and for biosensor application.

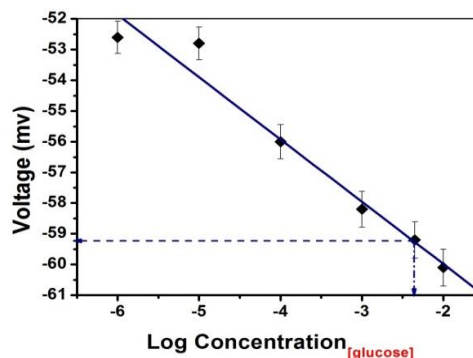


Fig. 7 Calibration curve for the potential difference between $Zn_{R}S$ as glucose biosensor electrode vs Ag/AgCl reference electrode in response to glucose concentrations in PBS, the glucose concentration in human blood plasma was marked at the x and y axis dashed curve.

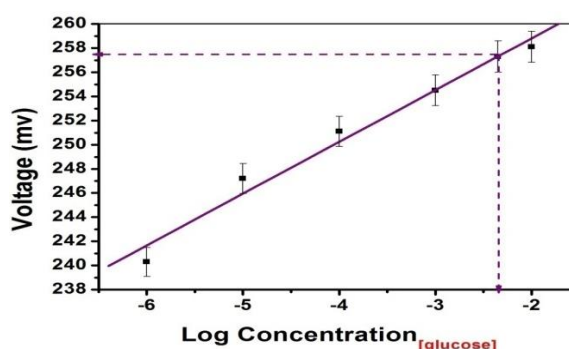


Fig. 8 Calibration curve showing the potential difference between $Zn_{R}T$ as glucose biosensor electrode vs Ag/AgCl reference electrode in response to glucose concentrations in PBS, the glucose concentration in human blood plasma was marked at the x and y axis dashed curve.

Figures (7&8) Show the Calibration curves for the potential difference between ($Zn_{R}S$ and $Zn_{R}T$ as glucose biosensor working electrodes versus the Ag/AgCl reference electrode in response to glucose concentrations in PBS, from the same curves we detected the glucose concentration in human blood plasma (dashed curves). While Tables (1 & 2) show the linear equations that represent calibration curves for glucose biosensors $Zn_{R}S$ and $Zn_{R}T$. From the results in the mentioned tables, the obtained experimental values are nearly the same as the theoretical values calculated from the linear equations (7 & 8).

$$Y = -2.028 X - 64.03 \quad (7) \text{ For } Zn_{R}S$$

$$Y = 4.28 X + 267.3 \quad (8) \text{ For } Zn_{R}T$$

The glucose concentration measurements for the two mentioned biosensors in PBS ranging from $1 \mu M$ to 10 mM show that the glucose dependence are linear with sensitivity slopes calculated from linear equation curves (5 & 6) equal to 64.03 and 267.3 mV/decades and the biosensors efficiency R^2 (regression coefficient) have a little bit difference, for glucose sensing see Table (1 & 2).

Table 1. The linear equation for ZN_RS biosensor calibration curve, R², Experimental and theoretical values.

Biosensor	X value (Log conc.)	Y (mV) (Exp. values)	Y(mV) (Theo. values)	R2
Silicon Electrode (ZN_RS) Eq. (5) Y= -2. 028 X - 64.03	-6	-52.6	-51.86	0.96
	-5	-52.8	-53.8	
	-4	-56	-55.9	
	-3	-58.2	-57.9	
	-2	-60.1	-59.9	

Table 2. The linear equation for ZN_RT biosensor calibration curve, R2, Experimental and theoretical values.

Biosensor	X value (Log conc.)	Y (mV) (Exp. values)	Y(mV) (Theo. values)	R2
Tip Electrode (ZN_RT) Eq. (6) Y= 4.28 X +267.3	-6	240.3	241.5	0.98
	-5	247.2	245.8	
	-4	251.1	250.1	
	-3	254.5	254.4	
	-2	258.1	258.7	

After successfully using the ZN_RS and ZN_RT for glucose concentration measurements in PBS, we can use them for the same measurement in the human blood plasma.

Tables (3 & 4) show the experimental obtained data for glucose concentrations in human blood plasma by using glucose biosensor- ZN_RS and ZN_RT, respectively according to calibration curves and the comparison with the theoretical data due to their linear equations and the results obtained from Accu-Chek Equipment for glucose concentrations measurements.

For ZN_RS glucose biosensor the measured potential responses were found to be equal to -59.2 mV in Y axis corresponding to -2.35 in X axis as marked in Table 3, which is equivalent to 4.4 m/l glucose concentration as detected from figure 5 this value is equal to 88 mg/dl glucose.

Moreover for ZN_RT glucose biosensor the measured potential responses were found to be equal to 257.3 mV

in Y axis corresponding to -2.36 in X axis as marked in Table 4, which is equivalent to 4.35 mM/l glucose concentration as shown in figure 6, this value is equal to 87 mg/dl glucose.

The obtain results are Consistent with the results obtained from Accu-Chek equipment for glucose detection, informing that the ZN_RS and ZN_RT glucose biosensor electrodes are highly sensitive to glucose concentration measurements.

The proposed biosensor stability and reproducibility were tested by using two mentioned biosensor kinds ZN_RS and ZN_RT glucose biosensor prepared separately using the same procedure. The relative standard deviation of the functionalized ZnO nano-rod -based glucose biosensor in human blood plasma was varying with less than 3%, which indicated a good reproducibility.

Table 3. Experimental, theoretical and Accu- Chek Equipment values for glucose concentration in human blood plasma using ZN_RS glucose biosensor.

Biosensor	Y (mV) (Exp. values)	Y (mV) (Theo. values)	X (log conc.) (Exp. values)	Conc. (Exp.)	Conc. (Accu - Chek)
Silicon Electrode	-59.21	-59.26	-2.35	4.4 mM/L	88 mg/dl
(Equation)				OR	
Y= -2.028X- 64.03				88 mg/dl	

Table 4. Experimental, theoretical and Accu- Chek Equipment values for glucose concentration in human blood plasma using ZN_RT glucose biosensor.

Biosensor	Y (mV) (Exp. values)	Y (mV) (Theo. values)	X (log conc.) (Exp. values)	Conc. (Exp.)	Conc. (Accu–Chek)
Tip Electrode	257.3	257.1	-2.36	4.35 mM/L	87 mg/dl
(Equation)				OR	
Y= 4.28 X + 267.3				87mg/dl	

4. Conclusions

The sol gel and aqueous chemical growth methods were succeeded in ZnO nano-rod thin film preparation deposited on two different substrate kinds, silicon (ZN_RS) and borosilicate glass capillary tube tip (0.5 and 0.7 μm as inner and outer diameters, respectively(ZN_RT) for glucose concentration measurements in both glucose stock solution (PBS) and in human blood plasma applications. The prepared films have hexagonal structure as revealed from XRD and FESEM analysis. ZnO nano-rods were found to be vertically aligned and distributed uniformly with diameter ranging from 22 up to 38 nm. The calibration curves of the logarithmic glucose concentration in PBS solution and in human blood plasma versus the output voltage response by using the mentioned biosensors, shows good linearity for a wide glucose concentration range with sensitivity slopes calculated from linear equation curves equal to -64.3 and 267.3 mV/decades and a regression coefficients R²= 0.96 and 0.98, respectively for glucose sensing.

For glucose concentration measurements in human blood plasma, the obtain results are consistent with the results obtained from Accu-Chek equipment as glucose detection ,indicating that the ZN_RS and ZN_RT biosensor electrodes are highly sensitive to glucose concentration measurements in extracellular solutions. In addition, ZN_RT glucose biosensor electrode is promising to be used as intracellular measurements due to its properties and very fine geometry can gently penetrate in the human cell without damaging it. The work is conduction for intracellular tip in the near future. We can conclude that by testing the prepared two ZN_RS and ZN_RT glucose biosensors prepared separately using the same procedure; we found that their relative standard deviation in human blood plasma was varying with less than 3%, which indicated a good reproducibility.

5. Conflict of Interest:

Authors declare that there is no conflict of interest

6. References

- [1] Ridhuan N S, Abdul Razak K and LockmanZ, Fabrication and Characterization of Glucose Biosensors by Using Hydrothermally Grown ZnO Nanorods, Scientific reports, 8, 13722 (2018).
- [2] Chou H. T., Lin J H., Hsu H. C., Wu T M. and Liu C., Bioelectrochemical properties of the ZnO nanorods modified by Au nanoparticles. Int. J. Electrochem. Sci, 10, 519–528 (2015).
- [3] Ibrahim M., Alaam, M. El-Haes H., Jalbout, A. F., de Leon A., , Analysis of the Structure and Vibrational Spectra of Glucose and Fructose, Ecl. Quim., Sao Paulo, 31(3), 15-21 (2005).
- [4] Ibrahim A., Elhaes H., Meng F., Ibrahim M.,Effect of Hydration on the Physical Properties of Glucose”, Biointerface Research in Applied Chemistry. 8 (4), 4114-4118, (2019).
- [5] Asif M. H., Danielsson B., Willander M., ZnO Nanostructure-Based Intracellular Sensor, Sensors,15, 11787-11804 (2015).
- [6] Jurablu S., Farahmandjou M., Firoozabadi T. P., Sol-Gel Synthesis of Zinc Oxide (ZnO) Nanoparticles: Study of Structural and Optical Properties, Journal of Sciences, Islamic Republic of Iran, 26, 281-285(2015).
- [7] Gurumurthy H., ZnO for performance enhancement of surface plasmon resonance biosensor: a review, Materials Research Express, 7, 012003 (2020).
- [8] Wahab H. A., Nur O., Willander M., Salama A. A., El Saeid A. A., Battisha I. K., Semiconductor ZnO Nano-Rods Thin Film Grown on Silver Wire for Hemoglobin Biosensor Fabrication, New Journal of Glass and Ceramics, 5, 9-15(2015).
- [9] Sarangi S. N., Nozaki S., Sahu S. N., ZnO Nanorod-Based Non-Enzymatic Optical Glucose, Biosensor, Journal of biomedical nanotechnology, 11, 988-96(2015).
- [10] Asif M. H., Ali S., Nur O., Willander M., Brännmark C., Strålfors P., Englund U., Elinder F., Danielsson B., FunctionalisedZnO-nanorod-based selective electrochemical sensor forintracellular glucose. Biosensors and Bioelectronics, 25, 2205–2211(2010).
- [11] Bagyalakshmi S., Sivakami A., Balamurugan K.S, A Zno nanorods based enzymatic glucose biosensor by immobilization of glucose oxidase on a chitosan film, Obesity Medicine, 18, 100229 (2020).
- [12] Cline G. W., Jucker B. M., Trajanoski Z., Rennings A. J. M., Shulman G. I., A novel 13C NMR method to assess intracellular glucose concentration in muscle, in vivo, American Journal of Physiology-Endocrinology And Metabolism, 274, E381–E389 (1998).

- [13] Yin Y. T., Que W. X., Kam C. H., ZnO Nanorods on ZnO Seed Layer Derived by Sol-Gel Process, *Journal of Sol-Gel Science and Technology*, 53, 605-612(2010).
- [14] Zak A. K., Abrishami M. E., Abd Majid W. H., Yousefi R., Hosseini S. M., Effects of Annealing Temperature on Some Structural and Optical Properties of ZnO Nanoparticles Prepared by a Modified Sol-Gel Combustion Method, *Ceramics International*, 37, 393-398(2011).
- [15] Wahab H. A., Nur O., Willander M., Salama A. A., El Saeid A. A., Battisha I. K., Optical, Structural and Morphological Studies of (ZnO) Nano-Rod Thin Films for Biosensor Applications Using Sol Gel Technique, *Resultin Physics*, 3, 46-51(2013).
- [16] Liu Z. F., Ya J., Lei E., Effects of Substrates and Seed Layers on Solution Growing ZnO Nanorods. *Journal of Solid State Electrochemistry*, 14, 957-963(2010).
- [17] Anusha J. R., Kim H. J., Fleming A. T., Das S. J., Yu K. H., Kim B. C., Raj C. J., Simple fabrication of ZnO/Pt/chitosan electrode for enzymatic glucose biosensor, *Sensors and Actuators B: Chemical*, 202, 827-833(2014).
- [18] Bagyalakshmi S., Karthick A., A Study on Enzymatic Electrochemical Glucose Biosensors Based on ZnO Nanorods, *International Journal of Scientific Research and Review*, 7,5(2020).
- [19] Scognamiglio V., Nanotechnology in glucose monitoring: advances and challenges in the last 10 years”, *Biosensors and Bioelectronics*, 47, 12-25(2013).
- [20] Wahab H. A., Nur O., Willander M., Salama A. A., El Saeid A. A., Battisha I. K., Growth of Zinc Oxide (ZnO) Nano-Rod Thin Film for Hemoglobin Biosensor Applications Prepared Using Sol-Gel and Aqueous Chemical Growth, *International Journal of Engineering and Innovative Technology (IJEIT)*, 4, 6-13(2014).
- [21] Arya A. K., Kumar L., Pukharia D., Tripathi K., Application of nanotechnology in diabetes, *Digest Journal of Nanomaterials and Biostructures*, 3, 221–225(2008).
- [22] Hilli S. M., Willander M., Öst A., Strålfors P., ZnO nanorods as an intracellular sensor for pH measurements, *Journal of Applied Physics*, 102, 084304–084305(2007).
- [23] Miao F., Lu X., Tao B., Li R. and Chu P K., Glucose oxidase immobilization platform based on ZnO nanowires supported by silicon nanowires for glucose biosensing., *Microelectron. Eng.*, 149, 153–158 (2016).
- [24] Asif M. H., Fulati A., Nur O., Willander M., Brännmark C., Strålfors P., Börjesson S. I., Elinder F., Functionalized zinc oxide nanorod with ionophore-membrane coating as an intracellular Ca²⁺ selective sensor, *Applied Physics Letters*, 95: 023703–023705(2009).
- [25] Ali S. M. U., Nur O., Willander M., Danielsson B., A fast and sensitive potentiometric glucose microsensor based on glucose oxidase coated ZnO nanowires grown on a thin silver wire, *Sensors and Actuators B*, 145, 869–874(2010).
- [26] Abe T., Lau Y. Y., Ewing A. G., Characterization of glucose microsensors for intracellular measurements, *Analytical Chemistry*, 64, 2160–2163(1992).
- [27] Yamada K., Nakata M., Horimoto N., Saito M., Matsuoka H., Inagaki N., Measurement of glucosdes uptake and intracellular calcium concentration in single, living pancreatic β -cells, *Journal of Biological Chemistry*, 275, 22278–22283(2000).
- [28] Asif M. H., Ali S. M., Nur O., Willander M., Englund U. H., Elinder F., Functionalized ZnO nanorod-based selective magnesium ion sensor for intracellular measurements. *Biosens. Bioelectron.*, 26, 1118–1123(2010)
- [29] Lahcen A. A., Rauf S., Beduk T., Durmus C., Aljedaibi A., Timu S., Alshareef H. N., Amine A., Wolfbeis O. S., Salama K. N., Hide details, *Electrochemical sensors and biosensors using laser-derived graphene: A comprehensive review*, *Biosensors and Bioelectronics*, 168, 15 (2020),
- [30] Asif M. H., Nur O., Willander M., Strålfors P., Brännmark C., Elinder F., Englund U. H., Lu J., Hultman L., Growth and structure of ZnOnanorods on a sub-micrometer glass pipette and their application as intracellular potentiometric selective ion sensor, *Materials*, 3, 4657–4667(2010).
- [31] Beduk T., Bihar E., Surya S. G., Castillo A. N., Inal S., Salama K. N., A paper-based inkjet-printed PEDOT:PSS/ZnO sol-gel hydrazine sensor, *Sensors and Actuators B: Chemical*, 306, (2020).
- [32] Wang Z. L., ZnO nanowire and nanobelt platform for nanotechnology, *Materials Science and Engineering: A*, 64, 33–71(2009).
- [33] Cui Y., Wei Q., Park H., Lieber C. M., Nanowire nanosensors for highly sensitive and selective detection of biological and chemical species, *Science*, 293, 1289–1292(2001).
- [34] Huang M. H., Mao S., Feick H., Yan H., Wu Y., Kind H., Weber E., Russo R., Yang P., Room-temperature ultraviolet nanowire nanolasers, *Science*, 292, 1897–1899(2001).
- [35] Li Q. H., Gao T., Wang Y. G., Wang T. H., Adsorption and desorption of oxygen probed from ZnO nanowire films by photocurrent measurements, *Applied Physics Letters*, 86, 123117–123119(2005)
- [36] Marzieh M., Iraj K., Optimising ZnO seed layer to improve the growth of the dense, aligned ZnO nanorods as an electron transport layer in perovskite solar cell applications, *Journal Materials Research Innovations*, 1, 1831144, (2020).